Effects of Chain Length and Au Spin-Orbit Coupling on $^3(\pi\pi^*)$ Emission from Bridging C_n^{2-} Units: Theoretical Characterization of Spin-Forbidden Radiative Transitions in Metal-Capped One-Dimensional Carbon Chains $[H_3PAu(C{\equiv}C)_nAuPH_3]$

Zexing Cao* and Qianer Zhang[a]

Abstract: Density functional theory and CASSCF calculations have been used to optimize the geometries of binuclear gold(I) complexes $[H_3PAu(C{\equiv}C)_nAuPH_3]$ ($n=1$–6) in their ground states and selected lowest energy $^3(\pi\pi^*)$ excited states. Vertical excitation energies obtained by time-dependent density functional calculations for the spin-forbidden singlet–triplet transitions have exponential-decay size dependence. The predicted singlet–triplet splitting limit of $[H_3PAu(C{\equiv}C)_\infty AuPH_3]$ is about 8317 cm^{-1}. Calculated singlet–triplet transition energies are in reasonable agreement with available experimental observations. The effect of the heavy atom Au spin-orbit coupling on the $^3(\pi\pi^*)$ emission of these metal-capped one-dimensional carbon allotropes has been investigated by MRCI calculations. The contribution of the spin- and dipole-allowed singlet excited state to the spin-orbit-coupling wave function of the $^3(\pi\pi^*)$ excited state makes the low-lying acetylenic triplet excited states become sufficiently allowed so as to appear in both electronic absorption and emission.

Keywords: ab initio calculations · carbyne ligands · density functional calculations · gold · spin-orbit coupling

Introduction

Transition-metal carbide clusters have growing interest in material science.[1] In particular, metal-capped carbon chains, $[L_mMC_nML_m]$, as the most fundamental class of carbon-rich molecular wires, have attracted considerable attention of numerous researchers in past few years.[2–13] Because physical and chemical properties of the carbon chain species both in the ground and in excited states may be significantly modified by an anticipated p_π–d_π bonding interaction between the alkynyl group and metal centers in the μ-C_n dinuclear organometallic compounds, these kinds of compounds have potential applications in molecular electronics, nonlinear optical materials, and molecular devices.[1]

Recently, a variety of μ-C_n-bridged binuclear complexes have been synthesized and their structures have been determined by spectroscopic and X-ray structural characterization.[2–4] Gladysz and co-workers[2] have synthesized the dirhenium homologues $[R(C{\equiv}C)_nR]$ ($n=4$–20; $R=(\eta^5\text{-}C_5Me_5)$-$Re(NO)(PPh_3)$). The effects of chain length on IR, Raman, NMR, and UV-visible spectra have been explored. On the basis of the UV-visible spectra, they suggested that the π–π* transition energy of rhenium-capped polyynediyl complexes has a linear relationship between the wavelength λ and $1/n$ ($n=$number of alkynyl units) as described by Hirsch and coworkers.[3] They estimated the limit of the lowest energy $^1(\pi\pi^*)$ absorption to be approximately 550 nm for the analogous bands at infinite chain length, irrespective of the endgroup.

The electronic and geometrical structures of C_n-bridged dinuclear complexes in their ground states have been investigated by theoretical calculations.[2,5–12] A qualitative Hückel-type scheme has been developed to predict the most appropriate valence structure.[12] The geometrical and bonding features at different oxidation states of few small bimetallic complexes have been clarified. For example, the interconversion of neutral polyynediyl and dication cumulenic valence structures in $[L_nReC_4ReL_n]^{n+}\,n\,[PF_6]^-$ has been confirmed by X-ray structural characterization in combination with natural bond-order analysis and topological electron-density calculations.[2]

Most recently, the $[Cy_3PAu(C{\equiv}C)_nAuPCy_3]$ ($n=1$–4) complexes have been synthesized by Che and co-workers.[13] These dinuclear gold(I) complexes bridged by C_n^{2-} show significant spectroscopic features of the triplet $^3(\pi\pi^*)$ excited

[a] Prof. Dr. Z. Cao, Prof. Q. Zhang
Department of Chemistry
State Key Laboratory for Physical Chemistry of Solid Surfaces
Xiamen University, Xiamen 361005 (China)
Fax: (+86) 592-2183047
E-mail: zxcao@xmu.edu.cn

DOI: 10.1002/chem.200305572

state. Both $^3(\pi\pi^*)$ emission and adsorption from bridging C_n^{2-} units are assumed to become sufficiently allowed through Au spin-orbit coupling to appear prominently. Such a heavy atom effect has been observed in unsaturated organic species.[14] In contrast to the spin-allowed π–π* excitation to the $^1(\pi\pi^*)$ excited state, the singlet–triplet excitation energy in the dinuclear gold(I) complexes follows linear relationship between λ^2 and n (n = number of alkynyl units), instead of linear dependence of λ on $1/n$ responsible for the singlet–singlet π–π* transition in rhenium-capped polyynediyls.[13]

Although it is known that the presence of heavy atoms can enhance the lifetime and emission quantum yield of intraligand triplet-excited states, knowledge of the geometrical and electronic structures of these states as well as fundamental aspects of the spin-orbit coupling is still sparse for such metal-capped wirelike polyynediyl chains. In order to understand the $^3(\pi\pi^*)$ emission from C_n^{2-} units, equilibrium geometries of these binuclear gold(I) complexes in their ground states and selected $^3(\pi\pi^*)$ excited states have been determined by density functional theory and ab initio electron correlation calculations, respectively. Singlet–triplet electron excitations and effect of the spin-orbit coupling (SOC) on the spin-forbidden transition are investigated.

Computational Methods

Density functional theory (DFT) calculations with the B3LYP[15,16] functional have been used to determine equilibrium geometries and vibrational frequencies of the $[H_3PAu(C{\equiv}C)_nAuPH_3]$ (n = 1–6) complexes. In DFT calculations performed with Gaussian 98 program,[17] the basis set used for the Au atoms was the double-zeta LANL2DZ in combination with the relativistic effective core potential (ECP) of Hay and Wadt,[18] augmented by an f polarization function. The standard 6-31G* basis set was employed for C, P, and H atoms. In time-dependent density functional theory (TD-DFT)[19] calculations, the 6-31G* basis set of C and P atoms was replaced by the cc-pvTZ basis set to improve the prediction of the excitation energies. In the calibration calculation for the $X\,^1\Sigma_g^+ \rightarrow {}^1\Sigma_u^+$ transition energy in HC_4H with a polyynediyl valence structure similar to the M-$(C{\equiv}C)_n$-M moiety, TD-DFT calculations predicted that the π–π* excited state $^1\Sigma_u^+$ lies at 8.16 eV above the ground state; this is comparable to the MRCI value of 8.02 eV and the CASPT2 value of 7.74 eV, as well as the experimental transition energy of 7.54 eV.[20] Previous calculations[21] showed that the $^1(\pi\pi^*)$ excited states of $HC_{2n}H$ with the polyynediyl structure are characterized by single excitations and TD-DFT calculations can predict reasonable excitation energies for these species with the polyynediyl valence structure. However, an adequate description of the excited state in this case requires involvement of quite a few orbitals and electrons in CASSCF and MRCI active spaces; this makes reliable MRCI and CASPT2 calculations unpractical for such wirelike systems containing heavy atoms.

Geometry optimization for selected $^3(\pi\pi^*)$ excited states of the dinuclear gold(I) compounds were performed by CASSCF calculations. We performed SOC calculations with the spin-orbit pseudopotential approach implemented with MOLPRO program package.[22] Reference wave functions used in SOC calculations were taken from MRCI calculations. In the CASSCF and MRCI calculations, the valence 6s and outer-core 5spd shells for Au were treated explicitly. The valence basis set of Au for the pseudopotential (ECP60MDF) with the spin-orbit potential parameters[23] were augmented by three f and two g polarization functions in SOC calculations. The spin-orbit potentials were used to predict accurate spectroscopic constants of AuX (X = F, Cl, Br).[23] The basis set for C, P, and H had double-zeta quality in the CASSCF and MRCI calculations. Oscillator strengths for an electronic transition were obtained from Equation (1):

$$f = {}^2/_3\Delta E|D|^2 \quad (1)$$

in which $\Delta E = E_a - E_b$ refers to the electronic energy difference in atomic units between the two states and D is the transition moment in atomic units.[24] The corresponding lifetime τ (in seconds) is given by Equation (2) in which $\tilde{\nu}$ is the transition energy in cm^{-1}.

$$\tau = \frac{3}{2f\tilde{\nu}^2} \quad (2)$$

Results and Discussion

Geometries and vibrational frequencies: B3LYP optimized geometries and vibrational frequencies of binuclear gold(I) complexes $[H_3PAu(C{\equiv}C)_nAuPH_3]$ (n = 1–6) (Scheme 1) in their ground states are presented in Table 1. DFT calculations predict that P–Au and Au–C bond lengths are about 2.34 and 1.98 Å, respectively; these values are close to those determined by X-ray structural analysis, that is, 2.287–2.292 Å and 2.000–2.012 Å, respectively, for $[(Cy_3P)Au(C{\equiv}C)_nAu(PCy_3)]$ (n = 1–3). Bond lengths of the C_n^{2-} bridge reveal that the ground state has triple and single bond alternation, whereby the C≡C bond length ranges from 1.223 to 1.236 Å and the C–C bond varies from 1.338 to 1.360 Å. Calculated C≡C bond lengths are slightly larger than the experimental values 1.17–1.20 Å, while calculated C–C bond lengths are generally smaller than the experimental values by 0.01–0.04 Å. It should be noted that the X-ray structures of the digold(I) compound indicate a small distortion of the

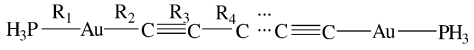

Scheme 1. Schematic drawing for the geometrical parameters in the $[H_3PAu(C{\equiv}C)_nAuPH_3]$ chain.

Table 1. B3LYP-optimized bond lengths and stretching frequencies of the C≡C bond in the C_n-bridged binuclear gold(I) complexes $[H_3P{-}Au{-}(C{\equiv}C)_n{-}Au{-}PH_3]$ (n = 1–6).

n	Geometries (R_1, R_2, ..)[a]			Frequencies[b]	
1	2.343	1.974	1.226	2037	
2	2.336	1.981	1.224	2034(111)	2156
	1.360				
3	2.336	1.982	1.226	2021	2128(55)
	1.351	1.223		2166	
4	2.336	1.977	1.232	2027(94)	2092
	1.351	1.232	1.344	2149	2183(10)
5	2.338	1.977	1.232	2017	2084(76)
	1.350	1.233	1.341	2086	2168
	1.235			2186(27)	
6	2.337	1.978	1.233	2013(44)	2038
	1.349	1.233	1.340	2078	2133
	1.236	1.338		2173(163)	2187

[a] R_1, R_2, .. (see Scheme 1) are bond lengths [Å]. [b] Vibrational frequencies [cm^{-1}] scaled by 0.96 and intensities [km mol] in parentheses.

linear carbon skeleton due to the strain effect from the bulky PCy_3 ligands and co-crystallized molecules. This slight distortion results in a more localized π-electron-bonding structure in $[(Cy_3P)Au(C{\equiv}C)_nAu(PCy_3)]$ than that in strictly linear $[H_3Au(C{\equiv}C)_nAuH_3]$ systems as their bond lengths show.

CASSCF optimized geometries of selected dinuclear gold(I) complexes in their singlet ground states and lowest-energy triplet $^3(\pi\pi^*)$ excited states are shown schematically in Figure 1. As the CASSCF-optimized bond lengths display,

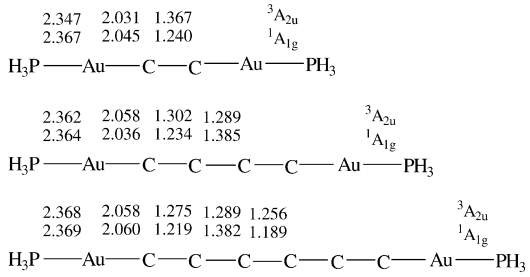

Figure 1. CAS(12,12)-optimized geometries of the singlet ground states and the triplet excited states.

the ground state has a triple and single bond alternate valence structure, while the triplet $^3(\pi\pi^*)$ excited state corresponds to a cumulenic structure with an equalization of the C–C bond length.

Frequency calculations for the ground states show that all wirelike structures with $[Au{-}(C{\equiv}C)_n{-}Au]$ (n = 1-6) moieties are stable on the potential-energy surfaces. Predicted C≡C bond stretch frequencies reasonably agree with available Raman observations for dinuclear gold(I) complexes. For instance, DFT predicts ν(C≡C) frequencies in $[H_3PAu(C{\equiv}C)_2AuPH_3]$ of 2034 and 2156 cm^{-1}, which can match Raman bands of 2087 and 2150 cm^{-1} in analogue $[(Cy_3P)Au(C{\equiv}C)_2Au(PCy_3)]$.[13]

Valence-shell ππ* excited states: The μ-C_n-bridged digold(I) complexes $[H_3PAu(C{\equiv}C)_nAuPH_3]$ in D_{3d} symmetry have the ground state $^1A_{1g}$. The π–π* electron excitation from the C_n units may give rise to low-lying states: $^{1,3}A_{2u}$, $^{1,3}A_{1u}$, $^{1,3}E_u$. Vertical transition energies of electron excitations to these $^{1,3}(\pi\pi^*)$ excited states are presented in Table 2. In comparison with available experimental values, TD-DFT calculations predict reliable singlet–triplet excitation energies for the $X^1A_{1g}{\rightarrow}^3(\pi\pi^*)$ transitions, and the deviation generally varies from −0.14 to −0.26 eV. For example, predicted triplet π–π* excited states $^3A_{2u}$, ^3E_u, and $^3A_{1u}$ of $H_3PAuC_2AuPH_3$ lie at 3.48, 3.66, and 3.85 eV, respectively, and they reasonably agree with the experimental bands at 331 nm (3.74 eV),

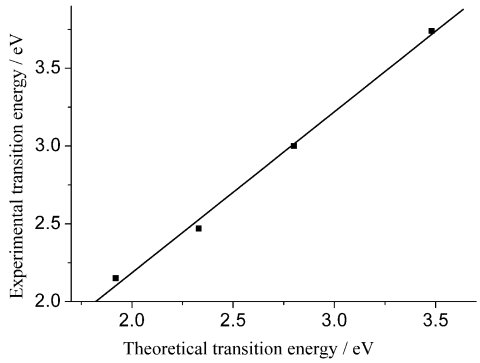

Figure 2. The predicted $X^1A_{1g}{\rightarrow}^3A_{2u}$ transition energies are correlated with the observed bands; see Equation (3) (R^2 = 0.996).

315 nm (3.93 eV), and 303 nm (4.09 eV).[13] As Figure 2 shows, there is an excellent correlation relationship between TD-DFT transition energies and observed bands for the electron excitation to the lowest triplet excited state $^3A_{2u}$, that is, Equation (3) holds in which A = 0.11432 eV, B = 1.0354.

$$T_{\text{exptl}} = A + BT_{\text{theor}} \quad (3)$$

Calculated results in Table 2 reveal that the spin-forbidden singlet–triplet transition energy decreases with an increase in the chain length, as observed in experiments.[13] To estimate the limit of the lowest energy $^3(\pi\pi^*)$ adsorption of $(C{\equiv}C)_{\propto}{}^{2-}$, an exponential-decay curve fitting has been examined on the basis of calculated vertical singlet–triplet transition energies (T_e in eV). The exponential-decay fitting gives Equation (4):

$$T_e = A + Be^{-n/C} \quad (4)$$

in which A = 0.88553, B = 3.50499, C = 3.32564, and n is the number of repeated C≡C units. The above analytic T_e–n expression reproduces the calculated results very well (Figure 3), and predicts the singlet–triplet splitting limit to be 0.88553 eV (7142 cm^{-1}) for $[H_3PAu(C{\equiv}C)_{\propto}AuPH_3]$. In consideration of the correlation relationship between theory and experiment defined in Equation (3), the modified limit is 1.0312 eV (8317 cm^{-1}). Such predicted singlet–triplet splittings of $(C{\equiv}C)_{\propto}{}^{2-}$ are comparable with the estimated limit of ~7000 cm^{-1} from experimental observations by Che and co-workers[13] combining the estimated $^1(\pi\pi^*)$ adsorption limit by Hirsch and co-workers.[3]

Table 2. Vertical transition energies (in eV) of the π–π* excitations in C_n-bridged binuclear gold(I) complexes $[H_3P{-}Au{-}(C{\equiv}C)_n{-}Au{-}PH_3]$ (n = 1–6).

n	$^1A_{2u}$	$^3A_{2u}$	$^1A_{1u}$	$^3A_{1u}$	^1E_u	^3E_u
1	4.44(0.895)[a]	3.48(3.74)[b]	3.85	3.85(4.09)[b]	3.88	3.66(3.93)[b]
2	4.02(1.302)	2.80(3.00)	3.35	3.35(3.43)	3.39	3.08(3.25)
3	3.84(1.823)	2.33(2.47)	3.02	3.02	3.07	2.68
4	3.70(2.594)	1.92(2.15)	2.68	2.68	2.73	2.30
5	3.58(3.641)	1.66	2.43	2.43	2.48	2.05
6	3.47(5.019)	1.47	2.23	2.23	2.27	1.86

[a] Oscillator strengths in parenthesis. [b] Experimental values in parenthesis for $[Cy_3PAu(C{\equiv}C)_nAuPCy_3]$ from reference [13].

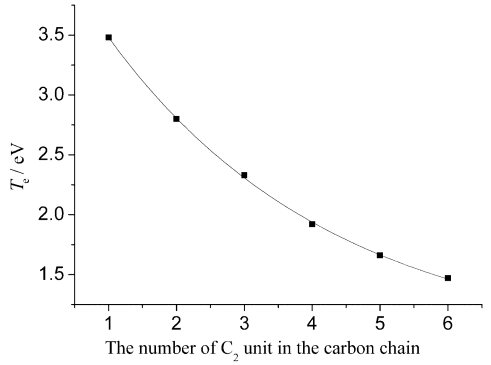

Figure 3. The size dependence of the $X^1A_{1g} \rightarrow {}^3A_{2u}$ transition energy; see Equation (4).

The triplet excited states $^3A_{1u}$ and ^3E_u arising from the π–π* excitation of the unsaturated carbon chain are slightly higher in energy than the $^3A_{2u}$. Analogous T_e–n patterns for the $^3A_{1u}$ and ^3E_u excited states can be seen in Table 2 in comparison with the $^3A_{2u}$ state.

The $^1A_{2u}$ excited state is the highest one of the acetylenic π–π* excited states in the digold(I)) polyynediyls. The spin-allowed $X^1A_{1g} \rightarrow {}^1A_{2u}$ transitions have the largest oscillator strengths. There is a notable singlet–triplet splitting between the $^1A_{2u}$ and $^3A_{2u}$ states, and this singlet–triplet spacing increases as the carbon chain extends. Calculated vertical excitation energies listed in Table 2 reveal a small energy gap between the ^1E_u and ^3E_u states, and the $^1A_{1u}$ and $^3A_{1u}$ states are almost isoenergetic. However, in comparison with corresponding $^1\Sigma_u^+ \rightarrow {}^3\Sigma_u^+$ energy gap in polyynes, the $^1A_{2u}$–$^3A_{2u}$ splitting is significantly reduced. For example, the energy difference between the singlet $^1\Sigma_u^+$ state and the triplet $^3\Sigma_u^+$ state in HC_4H is 4.69 eV by TD-DFT, while corresponding $^1A_{2u}$–$^3A_{2u}$ energy difference in [H_3PAu-C_4AuPH_3] is 1.22 eV. Such decrease of the $^1A_{2u}$–$^3A_{2u}$ energy difference in the μ-C_n-bridged digold(I) complexes may enhance the admixing of both states arising from the spin-orbit coupling, which plays an important role for the $^3(\pi\pi^*)$ emission (vide infra).

Singlet–triplet transitions: Emission and absorption spectra of digold(I) compounds [$(Cy_3P)Au(C{\equiv}C)_nAu(PCy_3)$] reveal that the lowest energy, electronically excited states are essentially acetylenic $^3(\pi\pi^*)$ in nature.[13] Present calculations on the π–π* excited states listed in Table 2 support this experimental consequence. The μ-C_n-bridged digold(I) complexes have a singlet ground state. Presumably, the spin-forbidden singlet–triplet transitions in digold(I) complexes become sufficiently allowed through Au spin-orbit coupling to appear observably.

Tables 3–5 summarize SOC calculations for the π–π* excited states. Calculations show that the "spin-forbidden" sinplet-triplet transitions have notable transition moments (TM) in magnitude, and they can occur as observed in experiments due to the presence of significant SOC interactions in the μ-C_n-bridged digold(I) complexes. For example, predicted transition moments for π–π* electron excitations to triplet excited states $^3A_{2u}$, ^3E_u, and $^3A_{1u}$ of [H_3PAu-C_2AuPH_3] are 0.001654, 0.02813, and 0.007769 au, respectively.

The effect of the heavy atom Au spin-orbit coupling on the singlet–triplet transition can be interpreted by the perturbation theoretical treatment. In a singlet–triplet transition the triplet wave function Ψ_T can be written as a series with perturbing states [Eq. (5)]:

Table 3. The composition [%] of the spin-orbit coupling wavefunction, scaled vertical transition energies (T_e in eV), transition dipole moments (DM in au), oscillator strengths (f), and lifetimes (τ in s) of the lowest triplet $^3(\pi\pi^*)$ state in [H_3P–Au–$(C{\equiv}C)_n$–Au–PH_3].

n	State	Composition	T_e[a]	DM	f [10^{-7}]	τ
1	$^3A_{2u}(m_s=\pm1)$	$^3A_{2u}(74.80)+{}^3A_{1u}(25.18)+{}^1A_{2u}(0.01)$	3.72	0.001654	2.4934	0.00668
2	$^3A_{2u}(m_s=\pm1)$	$^3A_{2u}(77.02)+{}^3A_{1u}(22.96)+{}^1A_{2u}(0.01)$	3.01	0.001484	1.6241	0.01564
3	$^3A_{2u}(m_s=\pm1)$	$^3A_{2u}(76.52)+{}^3A_{1u}(23.46)+{}^1A_{2u}(0.02)$	2.53	0.002230	3.0825	0.01168

[a] The splitting energies of $E[^3A_{2u}(m_s=0)]-E[^3A_{2u}(m_s=\pm1)$ are 488 cm^{-1} ($n=1$); 308 cm^{-1} ($n=2$); 226 cm^{-1} ($n=3$).

Table 4. The composition [%] of the spin-orbit coupling wavefunction, calculated vertical transition energies (T_e in eV), transition dipole moments (DM in au), oscillator strengths (f), and lifetimes (τ in s) of the triplet $^3A_{1u}$ state in [H_3P–Au–$(C{\equiv}C)_n$–Au–PH_3].

n	State	Composition	T_e[a]	DM	f [10^{-7}]	τ
1	$^3A_{1u}(m_s=\pm1)$	$^3A_{1u}(70.18)+{}^3A_{2u}(23.60)+{}^3E_u(m_s=0)(2.41)+{}^1E_u(3.76)$	3.85	0.007769	56.934	0.00027
2	$^3A_{1u}(m_s=\pm1)$	$^3A_{1u}(76.66)+{}^3A_{2u}(22.86)+E_u(ms=0)(0.15)+{}^1E_u(0.31)$	3.35	0.00152	1.8963	0.01083
3	$^3A_{1u}(m_s=\pm1)$	$^3A_{1u}(76.32)+{}^3A_{2u}(23.40)+{}^3E_u(m_s=0)(0.08)+{}^1E_u(0.18)$	3.02	0.00083	0.5097	0.049568

[a] The splitting energies of $E[^3A_{1u}(m_s=0)]-E[^3A_{1u}(m_s=\pm1)$ are -558 cm^{-1} ($n=1$); -437 cm^{-1} ($n=2$); -401 cm^{-1} ($n=3$).

Table 5. The composition [%] of the spin-orbit coupling wavefunction, calculated vertical transition energies (T_e in eV), transition dipole moments (DM in au), oscillator strengths (f), and lifetimes (τ in s) of the triplet ^3E_u state in [H_3P–Au–$(C{\equiv}C)_n$–Au–PH_3].

n	State	Composition	T_e[a]	DM	f [10^{-5}]	τ
1	$^3E_u(m_s=0)$	$^3E_u(58.27)+{}^1E_u(41.71)+{}^3A_{1u}(0.02)$	3.66	0.02813	7.09579	0.000024
2	$^3E_u(m_s=0)$	$^3E_u(61.11)+{}^1E_u(38.89)$	3.08	0.02171	3.55673	0.000068
3	$^3E_u(m_s=0)$	$^3E_u(61.61)+{}^1E_u(38.37)$	2.68	0.01781	3.1242	0.000103

[a] The splitting energies of $E[^3E_u(m_s=0)]-E[^3E_u(m_s=\pm1)$ are $-525/-1115$ cm^{-1} ($n=1$); $-251/-1031$ cm^{-1} ($n=2$); $-130/-1030$ cm^{-1} ($n=3$) for two components of ^3E_u.

$$\Psi_T = {}^3\Psi + \sum_S a_S {}^1\Psi_S + \sum_T a_T {}^3\Psi_T$$
$$a_i = \frac{\langle {}^3\Psi | H_{SO} | {}^1\Psi_i \rangle}{\Delta E} \quad (5)$$

in which the ΔE is the energy difference between ${}^1\Psi_i$ and ${}^3\Psi$. Evidently, the weight of the admixture a_i in Equation (5) is determined by both the spin-orbit matrix element $\langle {}^3\Psi | H_{so} | {}^1\Psi_i \rangle$ and the energy difference ΔE. As Table 2 shows, the singlet–triplet splittings among the $\pi\pi^*$ excited states in these dinuclear gold(I) complexes are generally small, and relevant singlet states can contribute to the triplet ${}^3(\pi\pi^*)$ excited states to some extent if the spin-orbit interaction becomes large. Due to the existence of the dipole-allowed singlet states in the SO wave functions of triplet ${}^3(\pi\pi^*)$ excited states, the triplet excited states can become sufficiently allowed to appear prominently in both electron adsorption and emission spectra.

Calculated lifetimes of the lowest triplet ${}^3(\pi\pi^*)$ excited states listed in Tables 3–5 reveal that triplet ${}^3(\pi\pi^*)$ excited states have relatively long lifetimes in the gas phase. For example, predicted lifetimes of the ${}^3A_{2u}$, ${}^3A_{1u}$, and ${}^3E_u$ excited states in $[H_3PAu(C{\equiv}C)_2AuPH_3]$ are 15.6 ms, 10.8 ms, and 68 μs, respectively. Such estimated lifetimes in the gas phase are larger than the observed lifetime of 10.8 μs for the ${}^3(\pi\pi^*)$ excited state of $[(Cy_3P)Au(C{\equiv}C)_2Au(PCy_3)]$ in the condensed phase in dichloromethane at room temperature. Calculated results in Tables 3–5 indicate that the energy splitting arising from the spin-orbit interaction between different m_s components of the ${}^3(\pi\pi^*)$ excited state gradually decreases as the chain increases.

Conclusion

Equilibrium geometries and vibrational frequencies of the metal-capped one-dimensional carbon chains $[H_3PAu(C{\equiv}C)_nAuPH_3]$ ($n = 1$–6) in their ground states have been determined by DFT calculations. Selected ${}^3(\pi\pi^*)$ excited states have been optimized by CASSCF calculations. Optimized bond lengths indicate that the ground states of such digold(I) compounds have a conjugated triple and single bond alternate bonding pattern, while the ${}^3(\pi\pi^*)$ excited states have the cumulenic valence structure. The spin-forbidden singlet–triplet transition energies, the corresponding oscillator strengths, and the lifetimes of the lowest ${}^3(\pi\pi^*)$ excited states have been determined. The vertical singlet–triplet transition energy has exponential-decay size dependence. As the chain increases, the singlet–triplet transition energy gradually converges to 7142 cm^{-1} (or 8317 cm^{-1}), which reasonably agrees with the value of ~7000 cm^{-1} suggested in previous study.[13] The coordination of Au^I to linear carbon chains will significantly lessen the singlet–triplet energy splitting and enhance the spin-orbit coupling in unsaturated carbon chains spanning two Au^I, which makes the lowest-energy ${}^3(\pi\pi^*)$ excited states become sufficiently allowed to appear prominently in both electronic adsorption and emission spectra.

Acknowledgement

This work was supported by the National Science Foundation of China (Project Nos. 20021002, 20173042 and 20233020) and the Ministry of Education of China. Z.C. gratefully acknowledges the Alexander von Humboldt Foundation for financial support during his stay at the University of Bonn and the Max-Planck Institute (MPI für Kohlenforschung, Mülheim an der Ruhr). Computational facilities provided by the department of theory of MPI are also acknowledged.

[1] a) U. H. F. Bunz, *Chem. Rev.* **2000**, *100*, 1605b) R. E. Martin, F. Diederich, *Angew. Chem.* **1999**, *111*, 1440; *Angew. Chem. Int. Ed.* **1999**, *38*, 1350; c) F. Paul, C. Lapinte, *Coord. Chem. Rev.* **1998**, *178–180*, 431; d) M. I. Bruce, *Coord. Chem. Rev.* **1997**, *166*, 91; e) M. A. Baldo, D. F. O'Brien, Y. You, A. Shoustikov, S. Sibley, M. E. Thompson, S. R. Forrest, *Nature* **1998**, *395*, 151; f) M. A. Baldo, M. E. Thompson, S. R. Forrest, *Nature* **2000**, *403*, 750; g) T. M. Swager, *Acc. Chem. Res.* **1998**, *31*, 201; h) N. D. Lang, P. Avouris, *Phys. Rev. B* **2000**, *62*, 7325.
[2] a) M. Brady, W. Weng, Y. Zhou, J. W. Seyler, A. J. Amoroso, A. M. Arif, M. Böhme, G. Frenking, J. A. Gladysz, *J. Am. Chem. Soc.* **1997**, *119*, 775; b) R. Dembinski, T. Bartik, B. Bartik, M. Jaeger, J. A. Gladysz, *J. Am. Chem. Soc.* **2000**, *122*, 810.
[3] G. Schermann, T. Grösser, F. Hampel, A. Hirsch, *Chem. Eur. J.* **1997**, *3*, 1105.
[4] N. L. Narvor, L. Toupet, C. Lapinte, *J. Am. Chem. Soc.* **1995**, *117*, 7129.
[5] D. R. Caulton, R. H. Cayton, R. H. Chisholm, J. C. Huffman, E. B. Lobkovsky, Z. Xue, *Organometallics* **1992**, *11*, 321.
[6] D. R. Neithamer, R. E. LaPointe, R. A. Wheeler, D. S. Richeson, G. D. Van Duyne, P. T. Wolczanski, *J. Am. Chem. Soc.* **1989**, *111*, 9056.
[7] J. Herdrich, M. Stelman, M. Appel, W. Beck, J. R. Phillips, W. C. Trogler, *Organometallics* **1990**, *9*, 1296.
[8] P. Belanzoni, N. Re, M. Rosi, A. Sgamellotti, C. Floriani, *Organometallics* **1996**, *15*, 4264.
[9] P. Belanzoni, N. Re, A. Sgamellotti, C. Floriani, *J. Chem. Soc. Dalton Trans.* **1998**, 1825.
[10] M. I. Bruce, P. J. Low, K. Costuas, J.-F. Halet, S. P. Best, G. A. Heath, *J. Am. Chem. Soc.* **2000**, *122*, 1949.
[11] a) H. Jiao, J. A. Gladysz, *New J. Chem.* **2001**, *25*, 551; b) H. Jiao, K. Costuas, J. A. Gladysz, J. Halet, M. Guillemot, L. Toupet, F. Paul, C. Lapinte, *J. Am. Chem. Soc.* **2003**, *125*, 9511.
[12] P. Belanzoni, N. Re, A. Sgamellotti, *J. Organomet. Chem.* **2002**, *656*, 156.
[13] a) C.M Che, H. Y. Chao, V. M. Miskowski, Y. Li, K. K. Cheung, *J. Am. Chem. Soc.* **2001**, *123*, 4985; b) W. Lu, H. F. Xiang, N. Zhu, C. M. Che, *Organometallics* **2002**, *21*, 2343.
[14] a) D. Li, X. Hong, C. M. Che, W. C. Lo, S. M. Peng, *J. Chem. Soc. Dalton Trans.* **1993**, 2929; b) X. Hong, K. K. Cheung, C. X. Guo, C. M. Che, *J. Chem. Soc. Dalton Trans.* **1994**, 1867.
[15] A. D. Becke, *J. Chem. Phys.* **1993**, *98*, 5648.
[16] C. Lee, W. Yang, R. G. Parr, *Phys. Rev. B* **1988**, *37*, 785.
[17] Gaussian 98 (Revision A.9), M. J. Frisch, G. W. Trucks, H. B. Schlegel, G. E. Scuseria, M. A. Robb, J. R. Cheeseman, V. G. Zakrzewski, J. A. Montgomery, Jr., R. E. Stratmann, J. C. Burant, S. Dapprich, J. M. Millam, A. D. Daniels, K. N. Kudin, M. C. Strain, O. Farkas, J. Tomasi, V. Barone, M. Cossi, R. Cammi, B. Mennucci, C. Pomelli, C. Adamo, S. Clifford, J. Ochterski, G. A. Petersson, P. Y. Ayala, Q. Cui, K. Morokuma, D. K. Malick, A. D. Rabuck, K. Raghavachari, J. B. Foresman, J. Cioslowski, J. V. Ortiz, A. G. Baboul, B. B. Stefanov, G. Liu, A. Liashenko, P. Piskorz, I. Komaromi, R. Gomperts, R. L. Martin, D. J. Fox, T. Keith, M. A. Al-Laham, C. Y. Peng, A. Nanayakkara, C. Gonzalez, M. Challacombe, P. M. W. Gill, B. G. Johnson, W. Chen, M. W. Wong, J. L. Andres, M. Head-Gordon, E. S. Replogle, J. A. Pople, Gaussian, Inc., Pittsburgh PA, **1998**.
[18] J. P. Hay, W. R. Wadt, *J. Chem. Phys.* **1985**, *82*, 299.
[19] M. E. Casida, C. Jamorski, K. C. Casida, D. R. Salahub, *J. Chem. Phys.* **1998**, *108*, 4439.

[20] T. Pino, H. Ding, F. Güthe, J. P. Maier, *J. Chem. Phys.* **2001**, *114*, 2208.
[21] C. Zhang, Z. Cao, H. Wu, Q. Zhang, *Int. J. Quant. Chem.* **2004**, *97*, in press.
[22] R. D. Amos, A. Bernhardsson, A. Berning, P. Celani, D. L. Cooper, M. J. O. Deegan, A. J. Dobbyn, F. Eckert, C. Hampel, G. Hetzer, P. J. Knowles, T. Korona, R. Lindh, A. W. Lloyd, S. J. McNicholas, F. R. Manby, W. Meyer, M. E. Mura, A. Nicklaß, P. Palmieri, R. Pitzer, G. Rauhut, M. Schütz, U. Schumann, H. Stoll, A. J. Stone R. Tarroni, T. Thorsteinsson, H.-J. Werner, MOLPRO; see www.tc.bham.ac.uk/molpro.
[23] M. Guichemerre, G. Chambaud, H. Stoll, *Chem. Phys.* **2002**, *280*, 71.
[24] S. D. Peyerimhoff, in *The Encyclopedia of Computational Chemistry, Vol. 4* (Eds.: P. von R., Schleyer, N. L. Allinger, T. Clark, J. Gasteiger, P. A. Kollman, H. F. Schaefer III, P. R. Schreiner), Wiley, Chichester, **1998**, pp. 2646 – 2664.

Received: September 25, 2003
Revised: November 27, 2003 [F5572]

